Theoretical Discussions on Electron Transport Properties of Perylene Bisimide Derivations with Different Molecular Packings and Intermolecular Interactions

Yun Geng,[a] Jianping Wang,[a] Shuixing Wu,[a] Haibin Li,[a] Fei Yu,[a] Guochun Yang,[a] Hongze Gao[b] and Zhongmin Su*,[a]

[a] *Institute of Functional Material Chemistry, Faculty of Chemistry, Northeast Normal University, Changchun 130024, P. R. China.*

[b] *Fundamental Department, Chinese People's Armed Police Force Academy, Langfang 065000, Hebei, P.R. China.*

Supplementary Information

Correspondence Address

Prof. Zhongmin Su

Institute of Functional Material Chemistry,

Faculty of Chemistry, Northeast Normal University,

Changchun 130024, People's Republic of China.

Fax: Fax: 86-431-85684009

E-mail Address: zmsu@nenu.edu.cn;

Evaluating Internal Reorganization Energy from Normal Mode Analysis

The contribution of each vibrational mode to reorganization energy can be obtained in the harmaonic approximation:

$$\lambda = \sum \lambda_i = \sum \hbar \omega_i S_i \tag{S1}$$

$$\lambda_i = \frac{k_i}{2} \Delta Q_i^2 \tag{S2}$$

where, ΔQ_i represents the displacement along normal mode i between the equilibrium geometries of the neutral and charged molecules. k_i is the corresponding force constant, S_i is the Huang-Rhys factor.

The site energy corrected method

The site energy corrected method proposed by Brédas is used to calculate the effective electronic coupling and effective site energies from the spatial overlap integral S_{ij}, electronic coupling V_{ij} and site energies $\varepsilon_{i(j)}$,

$$V_{12}^{eff} = \frac{V_{12} - \frac{1}{2}(\varepsilon_1 + \varepsilon_2) S_{12}}{1 - S_{12}^2} \tag{S3}$$

$$\varepsilon_{1(2)}^{eff} = \frac{1}{2} \frac{(\varepsilon_1 + \varepsilon_2) - 2V_{12}S_{12} \pm (\varepsilon_1 - \varepsilon_2)\sqrt{1 - S_{12}^2}}{1 - S_{12}^2} \tag{S4}$$

Assuming that H is the Hamiltonian of the dimer system and ψ_i and ψ_j are the highest occupied molecular orbitals (HOMO) of two monomers; S_{ij}, V_{ij}, and $\varepsilon_{i(j)}$ needed for the calculation of electronic coupling for p-type organic materials can be obtained from

$$S_{ij} = \langle \psi_i | \psi_j \rangle \tag{S5}$$

$$\varepsilon_i = \langle \psi_i | \hat{H} | \psi_i \rangle \tag{S6}$$

$$V_{ij} = \langle \psi_i | \hat{H} | \psi_j \rangle \tag{S7}$$

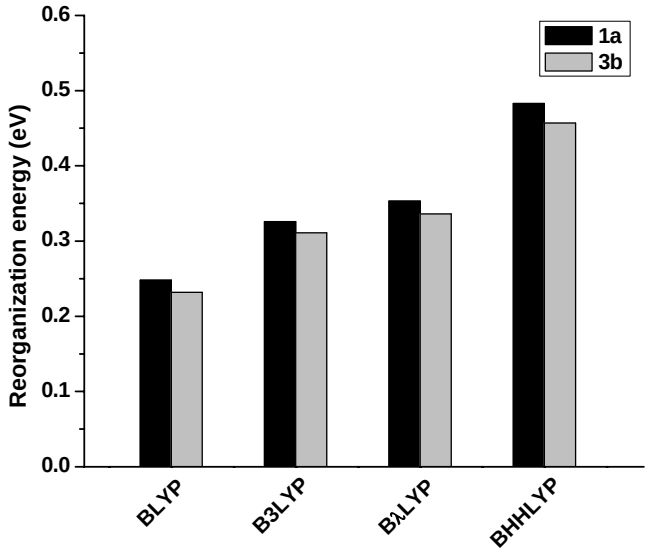

Fig. S1 Schematic description of the intramolecular reorganization energy of compound **1a** and **3b** calculated using different functionals, BLYP, B3LYP, BλLYP, and BHHLYP with the same basis set 6-31G(d,p).

Table S1 Bond lengths (Å), dihedral angles (°) and the lowest unoccupied molecular orbital (LUMO) energies (eV) in fully optimized geometry of **1a** and **3b** employing different functionals BLYP, B3LYP, BλLYP, BHHLYP with the 6-31G(d,p) basis set.

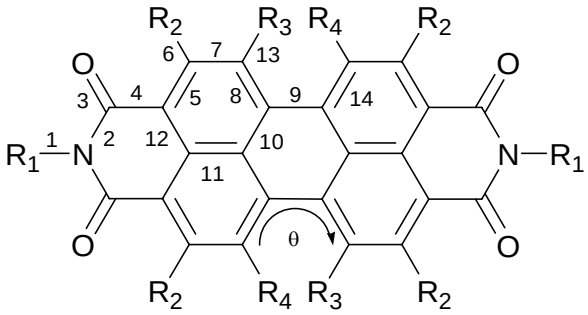

	1a					**3b**				
	BLYP	B3LYP	BλLYP	BHHLYP	Exp.	BLYP	B3LYP	BλLYP	BHHLYP	Exp.
1	1.023	1.014	1.012	1.005	0.880	1.473	1.460	1.460	1.450	1.467
2	1.403	1.389	1.387	1.375	1.379	1.421	1.406	1.404	1.391	1.399
3	1.231	1.217	1.215	1.202	1.226	1.235	1.221	1.218	1.205	1.211
4	1.501	1.493	1.493	1.486	1.525	1.491	1.483	1.483	1.477	1.487
5	1.411	1.398	1.396	1.383	1.389	1.391	1.378	1.378	1.364	1.369
6	1.751	1.732	1.731	1.717	1.702	1.090	1.084	1.081	1.075	0.950
7	1.432	1.425	1.424	1.419	1.429	1.400	1.393	1.393	1.388	1.387
8	1.409	1.395	1.392	1.379	1.376	1.415	1.400	1.397	1.383	1.392
9	1.479	1.474	1.475	1.471	1.494	1.474	1.469	1.470	1.467	1.472
10	1.437	1.426	1.425	1.417	1.414	1.447	1.437	1.436	1.428	1.436
11	1.433	1.420	1.417	1.404	1.414	1.445	1.432	1.430	1.417	1.428
12	1.443	1.432	1.431	1.423	1.380	1.426	1.416	1.415	1.407	1.410
13	1.756	1.738	1.737	1.722	1.721	1.367	1.351	1.349	1.336	1.409
14	1.409	1.395	1.392	1.379	1.384	1.415	1.401	1.398	1.385	1.390
θ	41.3	41.4	41.6	41.6	38.8	5.5	5.8	-6.2	-6.0	3.7
LUMO	-4.38	-4.16	-4.06	-3.31	-4.23	-4.01	-3.77	-3.65	-2.87	-3.88

[a]: Data from reference[19,26] cited in manuscript.

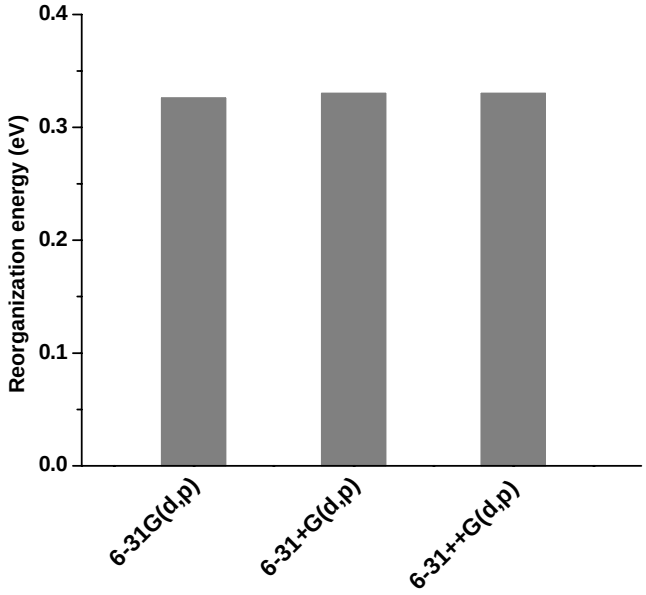

Fig. S2 Schematic description of the intramolecular reorganization energy of compound **1a** employing B3LYP functional and different basis sets (6-31G(d,p), 6-31+G(d,p), 6-31++G(d,p)).

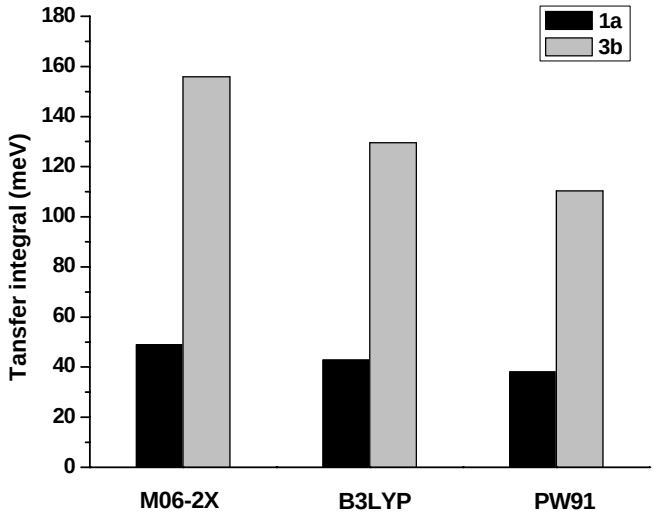

Fig. S3 The calculated transfer integrals employing different functionals, M06-2X, B3LYP and PW91, for representative hopping pathway (dimer A) of **1a** and **3b** respectively. The same basis set 6-31G(d,p) was selected.

Table S2 Bond lengths (Å) and dihedral angles (°) in fully optimized geometries based on B3LYP/6-31G(d,p), compared with experimental geometries.

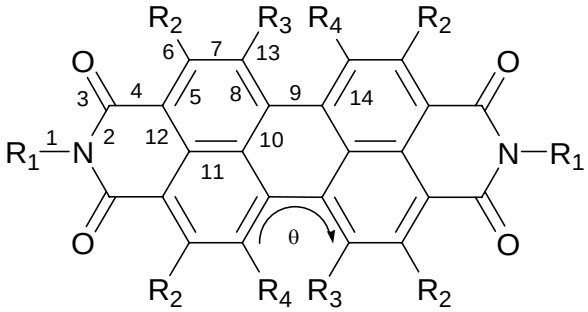

	1a		1b		2a		2b		2c		3a		3b	
	Cal.	Exp.	Cal.	Exp.	Cal.	Exp.	Cal.	Exp.	Cal.	Exp.	Cal.	Exp.	Cal.	Exp.
1	1.014	0.880	1.471	1.473	1.460	1.465	1.461	1.452	1.460	1.463	1.459	1.458	1.460	1.467
2	1.389	1.379	1.397	1.398	1.409	1.396	1.411	1.408	1.411	1.405	1.410	1.403	1.406	1.399
3	1.217	1.226	1.219	1.222	1.220	1.215	1.219	1.209	1.219	1.207	1.221	1.216	1.221	1.211
4	1.493	1.525	1.492	1.491	1.483	1.479	1.483	1.469	1.482	1.482	1.481	1.479	1.483	1.487
5	1.398	1.389	1.398	1.399	1.381	1.372	1.380	1.371	1.381	1.367	1.384	1.378	1.378	1.369
6	1.732	1.702	1.733	1.732	1.084	0.950	1.083	0.950	1.083	0.950	1.084	0.950	1.084	0.950
7	1.425	1.429	1.425	1.425	1.398	1.390	1.406	1.399	1.405	1.402	1.398	1.394	1.393	1.387
8	1.395	1.376	1.396	1.397	1.398	1.390	1.404	1.383	1.403	1.388	1.396	1.393	1.400	1.392
9	1.474	1.494	1.473	1.473	1.464	1.461	1.468	1.469	1.467	1.473	1.471	1.466	1.469	1.472
10	1.426	1.414	1.426	1.426	1.433	1.432	1.435	1.438	1.434	1.417	1.431	1.429	1.437	1.436
11	1.420	1.414	1.419	1.419	1.425	1.423	1.420	1.403	1.42	1.421	1.429	1.419	1.432	1.428
12	1.432	1.380	1.427	1.427	1.415	1.414	1.413	1.406	1.413	1.415	1.416	1.419	1.416	1.410
13	1.738	1.721	1.738	1.738	1.340	1.366	1.474	1.733	1.901	1.89	1.083	0.95	1.351	1.409
14	1.395	1.384	1.396	1.397	1.398	1.386	1.404	1.387	1.403	1.383	1.396	1.389	1.401	1.390
θ	41.4	35.8	40.7	40.7	25.0	25.3	35.6	36.0	36.1	37.2	0.6	1.5	5.8	3.7

Evaluating Classical Reorganization Energy

Firstly, the model systems for series **2** (a-c) and series **3** (a, b) shown in Fig. S1 were studied using quantum-chemical calculations to reduce the number of flexible degrees of freedom. While for series **1**, the model of **1b** is **1a**. The five model systems featured no substituent at the imide position. It is found that difference between computed geometries changes upon electron transfer is negligible. Due to the orbital occupation distributed mainly on the core, the frontier orbitals of model systems and real systems are also similar. The intramolecular reorganization energies of the model systems were calculated based on the same method with real systems, the results are

listed in Table S1. The difference λ_{con} between the reorganization energies of models and real systems can be attributed to the contributions of flexible substituents, which are mainly from low frequnency modes. So they can contribute to the classical reorganization energies.

Table S3 The reorganization energies of model systems and real systems, the contributions of flexible substituents and classical reorganization energies (eV).

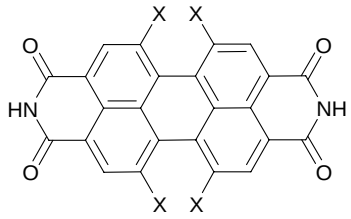

2a*: X=F
2b*: X=Cl
2c*: X=Br

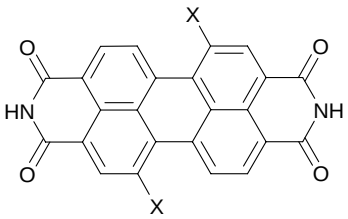

3a*: X=H
3b*: X=F

	1a*	**1b***	**2a***	**2b***	**2c***	**3a***	**3b***
λ_{in}	0.326	0.326	0.281	0.283	0.275	0.256	0.268
	1a	**1b**	**2a**	**2b**	**2c**	**3a**	**3b**
λ_{in}	0.326	0.330	0.321	0.318	0.308	0.298	0.311
λ_{con}		0.004	0.04	0.035	0.033	0.042	0.043
$\lambda_{classical}$	0.005	0.009	0.045	0.040	0.038	0.047	0.048

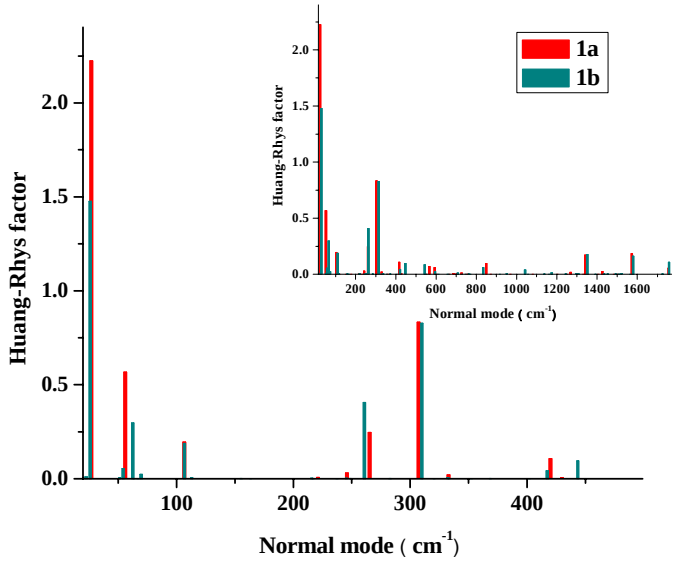

Fig. S4 The contributions of vibrations to the geometry relaxation for **1a** (red label) and **1b** (green label) respectively. The distributions in low frequency regions (below 500 cm^{-1}) are amplified, while the whole distributions are shown in the insert figure.

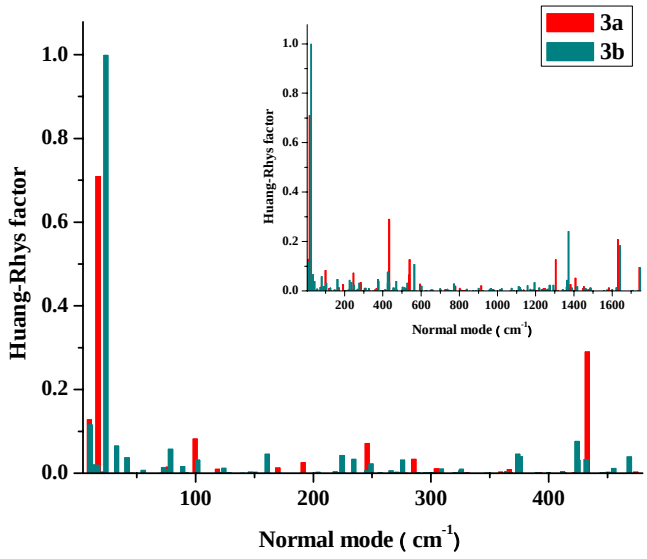

Fig. S5 The contributions of vibrations to the geometry relaxation for **3a** (red label) and **3b** (green label) respectively. The distributions in low frequency regions (below 500 cm^{-1}) are amplified, while the whole distributions are shown in the insert figure.

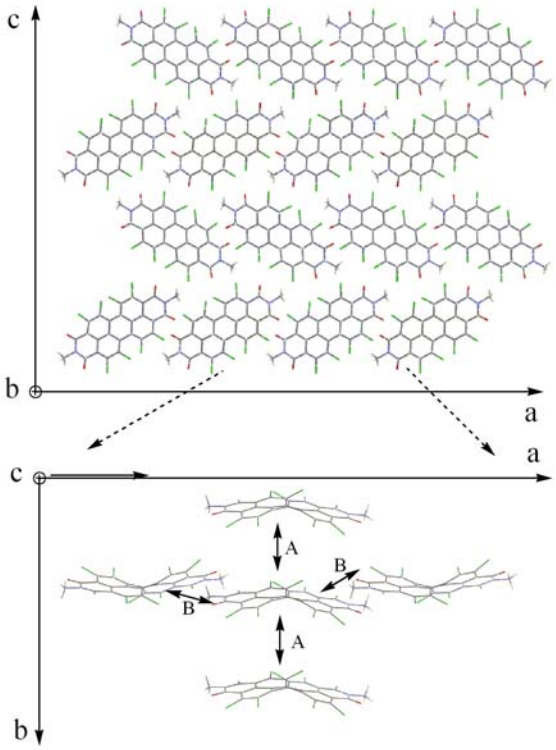

Fig. S6 Crystal of **1b**. (Top) An a-c plane of a 2×3×2 supercell structure; (Bottom) Main charge hopping pathways in a-b plane extracted from the supercell. According to the crystal symmetry of **1b**, the four main pathways can be assigned to two typical dimers *A* and *B* (for clarity, the solvent is omitted and only the perylene part is shown).

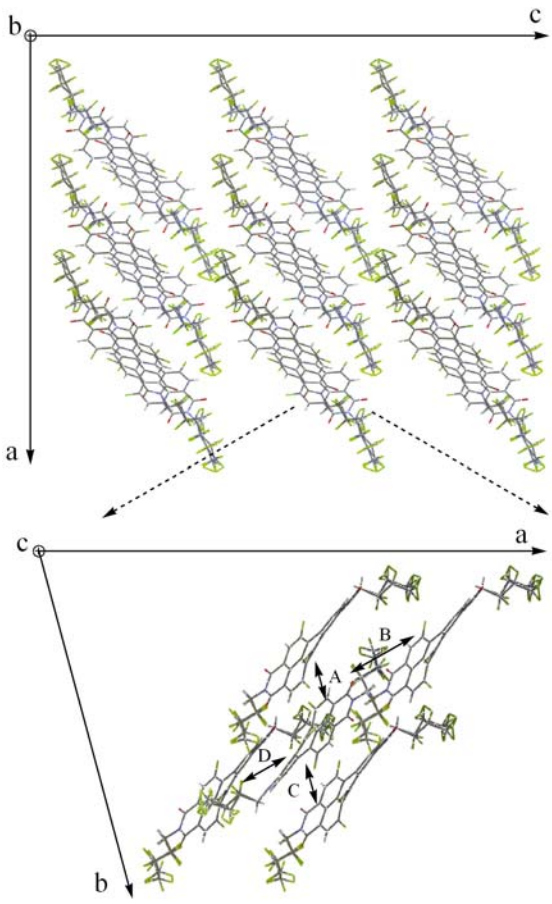

Fig. S7 Crystal of **2a**. (Top) An a-c plane of a 3×3×3 supercell structure; (Bottom) Main charge hopping pathways in a-b plane extracted from the supercell. According to alternating packing of two different enantiomers, four main pathways have four different types of dimmers *A*, *B*, *C* and *D*, respectively.

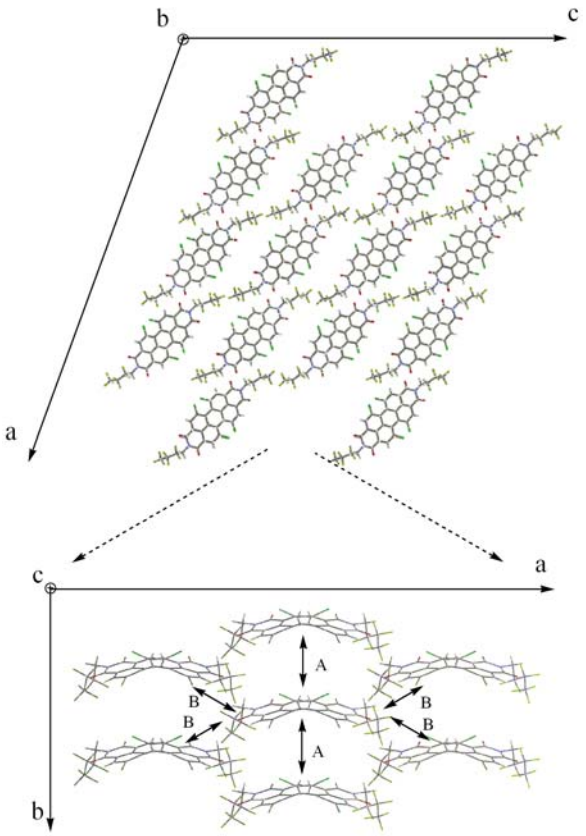

Fig. S8 Crystal of **2b**. (Top) An a-c plane of a 2×3×2 supercell structure; (Bottom) Main charge hopping pathways in a-b plane extracted from the supercell. According to the crystal symmetry of **2b**, the six main pathways can be assigned to two typical dimers *A* and *B* (for clarity, the solvent is omitted and only the perylene part is shown).

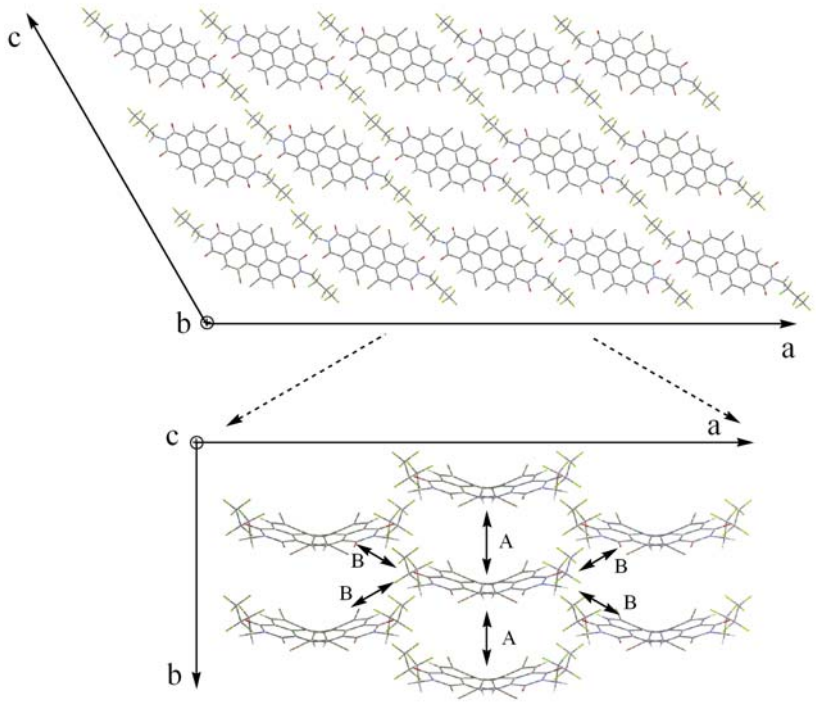

Fig. S9 Crystal of **2c**. (Top) An a-c plane of a 2×3×3 supercell structure; (Bottom) Main charge hopping pathways in a-b plane extracted from the supercell. According to the crystal symmetry of **2c**, the six main pathways can be assigned to two typical dimers *A* and *B* (for clarity, the solvent is omitted and only the perylene part is shown).

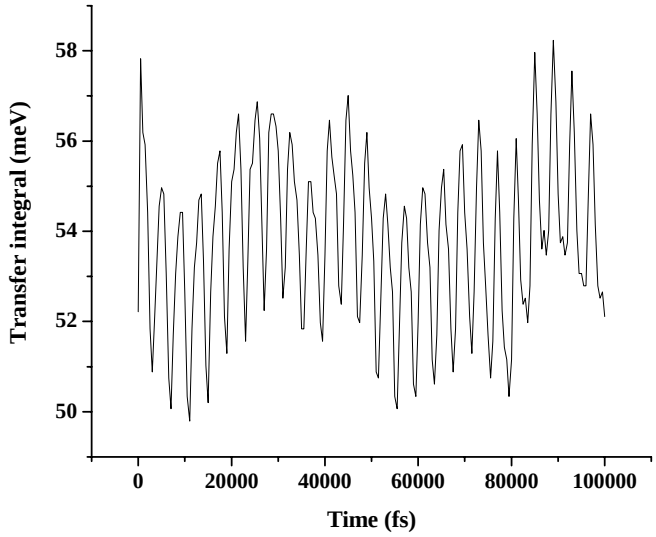

Fig. S10 Thermal fluctuation of the transfer integral of **1a** (dimer *A*) at 300 K.

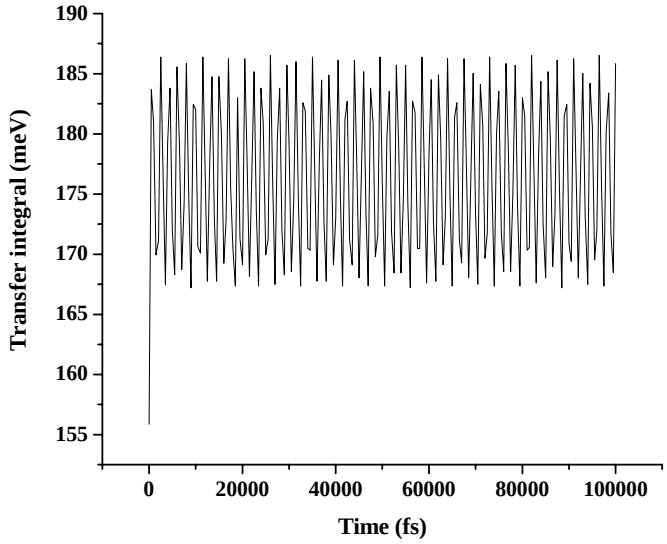

Fig. S11 Thermal fluctuation of the transfer integral of **3b** (dimer *A*) at 300 K.

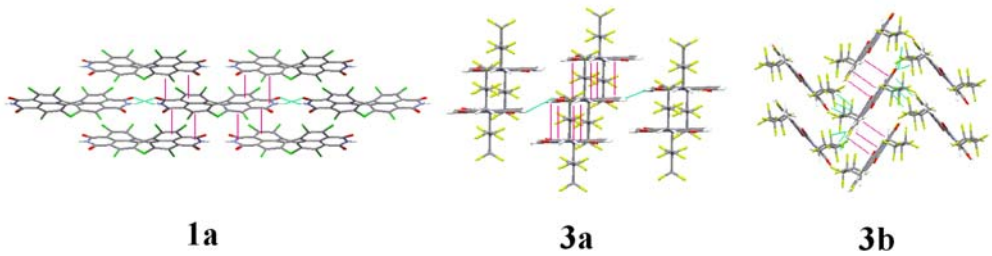

Fig. S12 Main intermolecular interactions for **1a**, **3a** and **3b**, the red represents π-π interaction and the green represents H-bond interaction or C-H…π interaction.

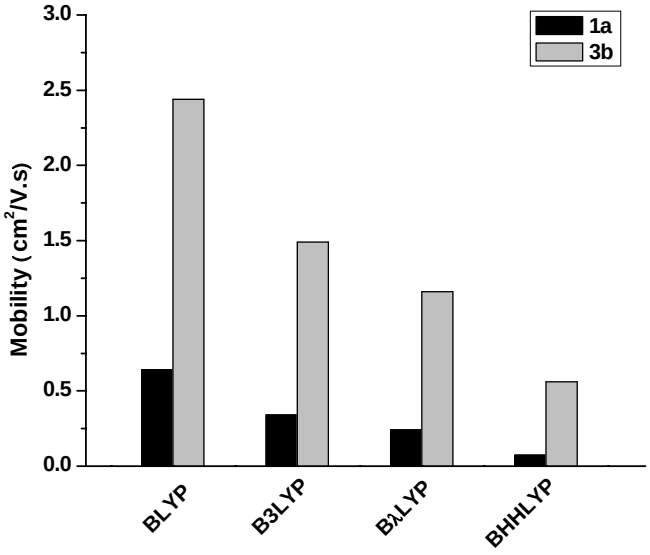

Fig. S13 The calculated electron mobilities of **1a** based on reorganization energies evaluated using different functionals, BLYP, B3LYP, BλLYP, and BHHLYP.